Micro-instability analysis of JET *H*-mode plasma during pellet fueling

P. Klaywittaphat[1] and T. Onjun[2]

[1]*Faculty of Engineering, Thaksin University, Phatthalung Campus 222 Moo. 2, Baan Prao Sub-District, Papayom District, Phatthalung, Thailand*

[2]*School of Manufacturing Systems and Mechanical Engineering, Sirindhorn International Institute of Technology, Thammasat University, Pathum Thani, Thailand*

1. Introduction

In this work, the impacts of pellets on the anomalous transport and micro-stability analysis of the drift electrostatic waves, specifically ITG and TEM modes, are investigated. A self-consistent simulation of JET *H*-mode discharge (discharge 53212) is carried out using the 1.5D BALDUR [1] integrated predictive modeling code. In this simulation, the pellet ablation is described using the neutral gas shielding (NGS) model with grad-*B* drift effect taken into account, which is a combination of an NCLASS neoclassical transport model and MMM95 anomalous transport model. The evolution of growth rate due to ITG and TEM modes is analyzed during the pellet fuelling operation. This can result in a better understanding of plasma behaviors during pellet injection.

2. Description of Models

2.1 MMM 95 anomalous transport model

The Multi-Mode model [2] is a combination of three theoretical based models, including the Weiland model for ion temperature gradient (ITG) and trapped electron modes (TEM), the Guzdar-Drake model for drift-resistive ballooning modes (RB), and a model for kinetic ballooning modes (KB). The thermal and particle transport coefficients can be expressed as [10]:

$$\chi_i = 0.8\chi_{i,ITG\&TEM} + 1.0\chi_{i,RB} + 1.0\chi_{i,KB} \quad (1)$$

$$\chi_e = 0.8\chi_{e,ITG\&TEM} + 1.0\chi_{e,RB} + 1.0\chi_{e,KB} \quad (2)$$

$$D_H = 0.8D_{H,ITG\&TEM} + 1.0D_{H,RB} + 1.0D_{H,KB} \quad (3)$$

$$D_z = 0.8D_{Z,ITG\&TEM} + 1.0D_{Z,RB} + 1.0D_{Z,KB}, \quad (4)$$

where χ_i is the ion thermal diffusion coefficient in the unit of m^2/s, χ_e is the electron thermal diffusion coefficient in the unit of m^2/s, D_H is hydrogenic particle diffusion coefficient in the unit of m^2/s and D_z is impurity particle diffusion coefficient in the unit of m^2/s.

2.2 NCLASS neoclassical transport model

Neoclassical ion thermal transport is computed using the NLASS module [4].

2.3 NGS ablation model and relocation model

During each pellet, two simultaneous processes, including pellet ablation and mass relocation, can take place. The neutral gas shielding (NGS) model [3] is used, in which an ablation rate of this model can be expressed in terms of the power function as follows:

$$\frac{dt}{dt} = 5.2 \times 10^{16} n_e^{0.333} T_e^{1.64} r_p^{1.333} M_i^{-0.333}, \quad (5)$$

where N, n_e (m^{-3}), T_e (eV), r_p (m), and M_i (u) are the number of particles in a pellet, electron density, electron temperature, pellet radius, and pellet mass, respectively. For the mass relocation model, a scaling model of pellet drift displacement, based on the grad-*B* induced pellet drift [5].

3. Micro-Instability Analysis

In this work, a JET *H*-mode discharge 53212 with high frequency pellet is considered. This discharge was a part of experiments undertaken at JET aimed to develop optimized pellet refueling scenarios. A high frequency pellet injector, which is capable of producing 4 mm^3 cubic pellets contains ~ 3.8 x 10^{21} D atoms and delivers them into plasma with the speed of 160 $m.s^{-1}$.

Table 1. Summary of equilibrium quantities for the three flux surfaces during pellet operation

Parameters	Time	n_e ($10^{20} m^{-3}$)	T_e (keV)	T_i (keV)	R/L_{ne}	R/L_{Te}	R/L_{Ti}	η_e	η_i	ν_{eff} (10^7)	β_e (10^{-3})
Dn/dr>0 (r=0.88)	t_0	0.5	1.40	1.25	23	12	11.2	1.92	2.05	0.15	6.5
	t_0+t_{abl}	0.55	1.42	1.30	-48	78	177	-0.62	-0.27	0.27	8.7
	t_0+50 ms	1.0	0.70	0.76	23	12	55	1.92	0.42	0.12	6.4
	t_0+75 ms	1.05	0.75	0.80	22.8	10	10	2.28	2.28	0.15	6.5
Dn/dr=0 r=0.93	t_0	0.5	1.18	1.12	30	13	12	2.31	2.50	0.15	4.5
	t_0+t_{abl}	2.5	0.18	0.17	0	35	51	0.00	0.00	2.2	4
	t_0+50 ms	0.85	0.65	0.70	40	12	25	3.33	1.60	0.2	3.95
	t_0+75 ms	0.8	0.58	0.65	41	10	9.5	4.10	4.32	0.3	4.1
Dn/dr<0 r=0.98	t_0	0.25	0.98	0.88	50	20	13	2.50	3.85	0.15	2.5
	t_0+t_{abl}	2.00	0.10	0.08	210	-180	-146	-1.17	-1.44	2.55	2.25
	t_0+50 ms	0.47	0.45	0.58	95	9	20	10.56	4.75	0.25	1.9
	t_0+75 ms	0.46	0.50	0.60	90	8	10	11.25	9.00	0.25	2

Figure 1 shows the time evolution of electron density, electron temperature, and ion temperature during pellet ablation. It can be seen that the electron density suddenly increases after pellet injection, but the electron and ion temperatures rapidly drop. It can also be seen that the maximum peaking density occurs around the peak of the pellet ablation profile (dn/dr=0). The micro-instability analysis for each of the flux surfaces is considered. In Figure 2, the top panel shows the radial locations selected for the micro-instability analysis, including ρ = 0.88, ρ = 0.93, and ρ = 0.98, which are the locations inside the peak of the pellet ablation profile, around the peak of the pellet ablation profile, and outside the peak of the pellet ablation profile, respectively. Some of the equilibrium information for micro instability analysis were obtained from BALDUR simulation. The values for these three surfaces mentioned the previous paragraph are summarized in Table 1.It can be seen that the micro

instability properties of the post-pellet profiles are highly sensitive to rapid and large excursions in the gradients, especially β_e and collisionality, in particular, at a location corresponding to the part of the pellet deposition profile. It is known that based on fluid concepts, an increase of the density gradient can stabilize the ion temperature gradient modes by decreasing the parameter $\eta_i = (\nabla T_i / T_i)/(\nabla n_i / n_i)$ However, in a gyrokinetic calculation for a density peaking case, it is found to be destabilizing [6]. Therefore, the stabilizing role of density peaking depends on the actual fraction of trapped electrons and plasma collisionality. An increase of α ($\alpha = -q^2 \beta R \nabla P / P$) can stabilize part of the micro turbulence [7].

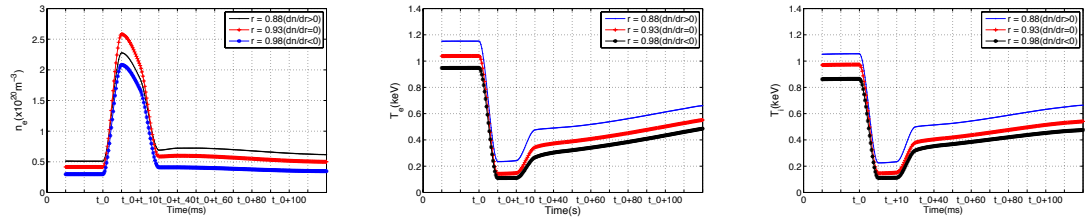

Figure 1. The time evolution of electron density, electron temperature and the ion temperature are shown during pellet ablation.

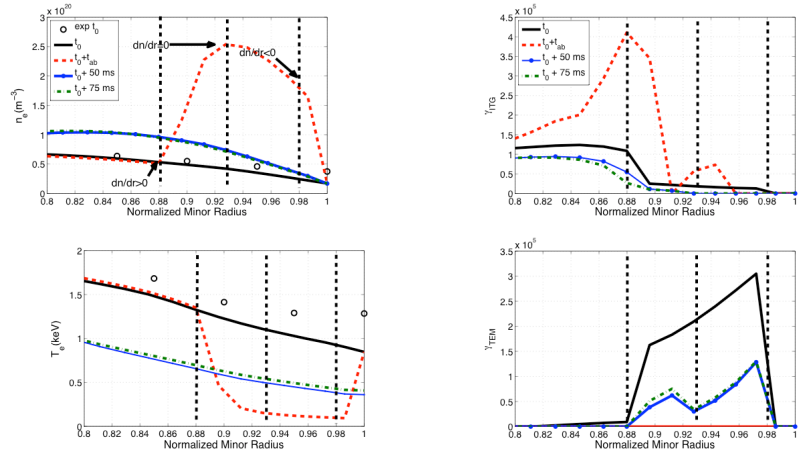

Figure 2. (Left) The profiles of electron density and electron temperature during the pellet fueling operation are shown for the radius from ρ = 0.8 to ρ = 1.0.

Figure 3. (Right) The profiles of the growth rate due to ITG and TEM during the pellet fueling operation are shown for the radius from ρ = 0.8 to ρ = 1.0.

Figure 3 shows that the maximum growth rate for ITG and TEM modes during the pellet injection obtained from the simulation using the MMM95 transport code. At dn/dr > 0 (r=0.88) the ITG growth rate is increased immediately after pellet injection t_0+t_{abl}. The ITG modes can be stabilized by the increased density gradient and the decreased ion temperature gradient, however, at this time the strong increase of ion temperature gradient tends to destabilize ITG growth rate. For the trapped electron modes (TEM) immediately after pellet injection (t_0+t_{abl}). The TEM growth rate is decreased due to an increase of electron

collisionality. Then, the growth rate recovers to the primary state at the middle location of the peak due to the pellet ablation profile, where $dn/dr \approx 0$ (r=0.93). Immediately after pellet injection t_0+t_{abl}, we observe an initial decrease in the growth rate of TEM and a simultaneous increase of the growth rates of ITG. At this time electron collisionality increases significantly, which suppresses the TEM growth rates. During the relaxation of the pellet deposition profile ($t = t_0$+50 ms), the growth rate based on TEM increases from the previously time while the growth rate based on ITG mode drops at this time, and at $t = t_0$+50 ms all profiles recover to the first state. At the outer surface with $dn/dr < 0$ (r=0.98), after the pellet ablation (at $t = t_0$ +50 ms), there is a reduction of the growth rates and the complete stabilization of modes ITG and TEM. This suggests that in lower collisionality plasmas, the post-pellet may be unstable to TEM and ITG. It can also be seen that ITG modes, which dominate before pellet injection, are increased by the increased temperature gradient, and TEM modes are stabilized by increased collisionality during pellet injection.

5. Conclusions

The time evolution of a JET *H*-mode plasma discharge 53212 is simulated using BALDUR integrated predictive modeling code, and a micro-instability analysis during pellet injection is carried out. A strong perturbation on the plasma causing a sudden change of thermal and particle transports can be observed after each pellet enters the plasma. This perturbation due to each pellet results in a change in both thermal and particle transport, especially on the resistive ballooning modes due to the increase of collisionality and resistivity near the plasma edge. The results show that the micro-instability properties of the post-pellet profiles are highly sensitive to rapid and large excursions in the gradients, β_e and collisionality, induced by the pellet injection. In particular, at a location, corresponding to the part of the pellet deposition profile, ITG modes are destabilized by an increase of temperature gradient, and TEM modes are stabilized by increased collisionality.

Reference

[1] C E Singer et al. 1988, Comput. Phys. Commun. **49** 275

[2] G Bateman et al. 1998 Physics of Plasmas **5** 1793

[3] P B Parks et al. 1978 Phys. Fluids **21** 1735

[4] W A Houlberg, et al. 1997 Phys. Plasma **4** 3230

[5] F Köchl et al. in Proc. 35th EPS Conf. Plasma Phys. 32D P-4.099, 9–13 June 2008, Hersonissos, Greece, 2008

[6] M Romanelli et al. 2004 Phys. Plasmas **11** 3845

[7] C Bourdelle et al. 2005 Nucl. Fusion **45** 110